Magnetic properties of $Nd_{0.9}Dy_{0.1}Fe_3(BO_3)_4$

A.A. Demidov [a,*], I.A. Gudim [b], E.V. Eremin [b]

[a] *Bryansk State Technical University, 241035 Bryansk, Russia*
[b] *Kirensky Institute of Physics, Russian Academy of Sciences, 660036 Krasnoyarsk, Russia*

ARTICLE INFO

ABSTRACT

The magnetic properties of trigonal $Nd_{0.9}Dy_{0.1}Fe_3(BO_3)_4$ substituted compound with the competitive Nd–Fe and Dy–Fe exchange interactions have been investigated. It has been shown that in $Nd_{0.9}Dy_{0.1}Fe_3(BO_3)_4$ a spontaneous spin-reorientation transition from an ease-axis state to an easy-plane occurs near 8 K. Anomalies of the magnetization curves are observed in a spin-flop transition induced by the magnetic field B∥c. The calculations were performed using a molecular-field approximation and a crystal-field model for the rare-earth subsystem. Extensive experimental data on the magnetic properties of $Nd_{0.9}Dy_{0.1}Fe_3(BO_3)_4$ have been interpreted and good agreement between theory and experiment has been achieved using the obtained theoretical dependences.

© 2011 Elsevier B.V. All rights reserved.

1. Introduction

$Nd_{0.9}Dy_{0.1}Fe_3(BO_3)_4$ compound belongs to the family of rare-earth ferroborates $RFe_3(BO_3)_4$ (space group R32), which exhibits a variety of phase transitions and some multiferroic features [1–3]. The iron subsystem in these compounds orders antiferromagnetically with the Neel temperature in the interval 30–40 K. The rare-earth subsystem is magnetized due to f–d coupling. The intrinsic anisotropy of iron subsystem tends to orientate the magnetic moments in the basal plane. The resulting magnetic structure depends on the rare-earth subsystem, the magnetic anisotropy of which is formed by the crystal-field.

For $DyFe_3(BO_3)$ the magnetic moments of both subsystems are directed along the trigonal axis c at $T < T_N \approx 39$ K [4–6]. In $DyFe_3(BO_3)$ at the magnetic field along the trigonal axis for $T < T_N$ a spin-flop transition occurs in the iron subsystem, the iron magnetic moments change their direction from the trigonal axis to basal plane by jump. This reorientation is accompanied by the orientation of rare-earth magnetic moments along the magnetic field direction [5]. For $NdFe_3(BO_3)_4$ at $T < T_N \approx 31$ K all the magnetic moments are lying in the basal plane. Magnetization curves of $NdFe_3(BO_3)_4$ are more complicated due to the existence of domain structure of this trigonal easy-plane antiferromagnet. However, a spin-flop transition occurs at the magnetic field in the basal plane ~1 T in one of three possible domains [4,7–10]. The $Nd_{1-x}Dy_xFe_3(BO_3)_4$ compounds exhibit spontaneous and induced external magnetic field spin-reorientation transitions produced

by competition of various contribution of the Nd^{3+} and Dy^{3+} ions in magnetic anisotropy [11–13]. It has been shown that the antiferromagnetic state in $Nd_{0.75}Dy_{0.25}Fe_3(BO_3)_4$ below the Neel temperature is easy-plane and a spontaneous spin-reorientation transition to an uniaxial state occurs near 25 K [11–13].

In this paper the experimental and theoretical investigations of the magnetic properties of $Nd_{0.9}Dy_{0.1}Fe_3(BO_3)_4$ have been performed.

2. Experiment

The single crystals have been grown from 300 g flux based on trimolibdate bismuth 75%mass.$[Bi_2Mo_3O_{12}+3B_2O_3+0.54Nd_2O_3+0.06Dy_2O_3]+25\%$mass.$Nd_{0.9}Dy_{0.1}Fe_3(BO_3)_4$ using the procedure particularly described in [12]. Saturation temperature was 980 ± 3 °C. The crystallization interval was 7 °C. Magnetic measurements were performed using the physical properties measurement system PPMS-9 (Quantum Design). The temperature interval was 2–300 K in magnetic fields up to 9 T. All magnetic measurements were performed with the external magnetic field either parallel or perpendicular to the c axis of the crystal. In comparison with [12] this paper presents new experimental data: the magnetization in the basal plane $M_{\perp c}(B)$, the magnetization along the c axis $M_c(B)$ at $T = 5, 7, 10, 20$ K, data of $M_c(B)$ for $B = 5$–9 T and data of initial magnetic susceptibility $\chi_{c,\perp c}(T)$ at $T = 50$–300 K.

3. Theory

The magnetic properties of $Nd_{1-x}Dy_xFe_3(BO_3)_4$ crystals are determined both by the magnetic subsystems and by the

interaction between them. The iron subsystem in this compound can be considered as consisting of two antiferromagnetic sub-lattices. The rare-earth subsystem (magnetized due to the f–d interaction) can also be represented as a superposition of two sublattices. In the calculations we used a theoretical approach which has been successfully applied for description of the magnetic properties of the $RFe_3(BO_3)_4$ (see e.g. [3,5,8,14–17]). This approach is based on a crystal-field model for the rare-earth ion and on the molecular-field approximation. Effective Hamiltonians describing the interaction of each R/Fe ion in the ith ($i=1, 2$) sublattice of the corresponding subsystem in the applied magnetic field B can be written as

$$\mathscr{H}_i(R) = \mathscr{H}_i^{CF} - g_J^R \mu_B J_i^R [B + \lambda_{fd}^R M_i^{Fe}], \quad (1)$$

$$\mathscr{H}_i(Fe) = -g_S \mu_B S_i [B + \lambda M_j^{Fe} + (1-x)\lambda_{fd}^{Nd} m_i^{Nd} + x\lambda_{fd}^{Dy} m_i^{Dy}], \quad j=1,2, j\neq i, \quad (2)$$

where $\mathscr{H}_i^{CF}$ is the crystal-field Hamiltonian, g_J^R is the Lande factor, J_i^R is the operator of the angular moment of the R ion, $g_S=2$ is the g-value, S_i is the operator of the spin moment of the iron ion and $\lambda_{fd}^R < 0$ and $\lambda < 0$ are the molecular constants of the AFM interactions (R–Fe and Fe–Fe, respectively). The magnetic moments of the ith iron M_i^{Fe} and rare-earth m_i^R sublattices per formula unit are determined by the relationships

$$M_i^{Fe} = 3g_S \mu_B \langle S_i \rangle, \quad m_i^R = g_J^R \mu_B \langle J_i^R \rangle \quad (3)$$

The crystal-field Hamiltonian $\mathscr{H}^{CF}$ can be expressed using irreducible tensor operators C_q^k as

$$\mathscr{H}^{CF} = B_0^2 C_0^2 + B_0^4 C_0^4 + B_3^4(C_{-3}^4 - C_3^4) + B_0^6 C_0^6 + B_3^6(C_{-3}^6 - C_3^6) + B_6^6(C_{-6}^6 - C_6^6) \quad (4)$$

For Nd^{3+} and Dy^{3+} ions in $Nd_{0.9}Dy_{0.1}Fe_3(BO_3)_4$, the crystal-field parameters B_q^k are unknown and data on the splitting of the ground-state multiplet are unavailable.

In order to calculate the magnitudes and orientations of magnetic moments in the iron and rare-earth subsystems, it is necessary to solve a self-consistent problem based on Hamiltonians (1,2) under the condition of minimum for the corresponding thermodynamic potential (see e.g. [3,14]). Then, it is possible to determine the regions of stability of various magnetic phases, the critical fields for the phase transitions, the magnetization curves, magnetic susceptibilities, etc.

The magnetization and magnetic susceptibility of the compound (per f.u.) are defined as

$$M = \frac{1}{2}\sum_{i=1}^{2}(M_i^{Fe} + (1-x)m_i^{Nd} + xm_i^{Dy}),$$

$$\chi_k = \chi_k^{Fe} + (1-x)\chi_k^{Nd} + x\chi_k^{Dy}, \quad k=a,b,c. \quad (5)$$

In the ordered phase, the initial magnetic susceptibility of the compound under consideration can be determined using the initial linear portions of the magnetization curves calculated for the corresponding directions of the external magnetic field. In the paramagnetic phase, where the interactions between rare-earth and iron subsystems can be ignored, the magnetic susceptibility of the rare-earth subsystem can be determined using the well-known Van Vleck formula for the energy spectrum and wave functions calculated on the basis of the crystal-field Hamiltonian (4). For the iron subsystem, the susceptibility can be described in terms of the Curie–Weiss law (with the corresponding paramagnetic Neel temperature Θ).

4. Results and discussion

For the calculation of the magnetic characteristics of $Nd_{0.9}Dy_{0.1}Fe_3(BO_3)_4$ compound in an external magnetic field directed parallel and perpendicular to the trigonal axis c with inclusion of the possible easy-axis and easy-plane states of the magnetic subsystem of the compound, we used the schemes of orientations of the magnetic moments of the iron M_i^{Fe} and rare-earth m_i^R sublattices (Fig. 1). The calculations of the magnetic characteristics according to schemes (a) and (b) were performed for the magnetic field directed along the trigonal axis c, i.e., $B\|c$. Schemes (c) and (d) were used for the case of the orientation of the magnetic field in the basal plane, i.e., $B\perp c$. Fig. 1 also shows the directions of the net magnetic moments of the rare-earth subsystem $m_{1,2} = (1-x)m_{1,2}^{Nd} + xm_{1,2}^{Dy}$, as well as their projections (m_{ic} and m_{ia}) along the field direction.

In order to determine the parameters of a crystal-field B_q^k, we have used the experimental data on the temperature dependence of the initial magnetic susceptibility of $Nd_{0.9}Dy_{0.1}Fe_3(BO_3)_4$ measured in the paramagnetic state (from $T_N \approx 31$ K to 300 K) along the trigonal axis and in the basal plane. The best agreement is achieved for the following set of the crystal-field parameters ($B_q^k = Nd[Dy]$, in cm^{-1}):

$$B_0^2 = 597[626], \, B_0^4 = -1361[-1300], \, B_3^4 = 750[-723],$$

$$B_0^6 = 585[696], \, B_3^6 = 140[-60], \, B_6^6 = 410[-283]. \quad (6)$$

Analysis of the experimental data and performed calculations showed, that in $Nd_{0.9}Dy_{0.1}Fe_3(BO_3)_4$ at low temperatures and when $B=0$, the magnetic moments of the $Nd_{0.9}$, $Dy_{0.1}$ and Fe-subsystems are oriented along the trigonal axis c (collinear phase, scheme (a) in Fig. 1). For an antiferromagnetic ordering of the magnetic moments of the iron subsystem along the trigonal axis for $B\|c$ at $T=2$ K, this subsystem does not contribute to the magnetization (because of a small parallel susceptibility) and, hence, the initial part of $M_c(B)$ can be used for selecting λ_{fd}^R (to which the magnetization curve in this region is highly sensitive). For $B > B_{SF}$ (B_{SF} is the spin-flop transition field), the slope of the
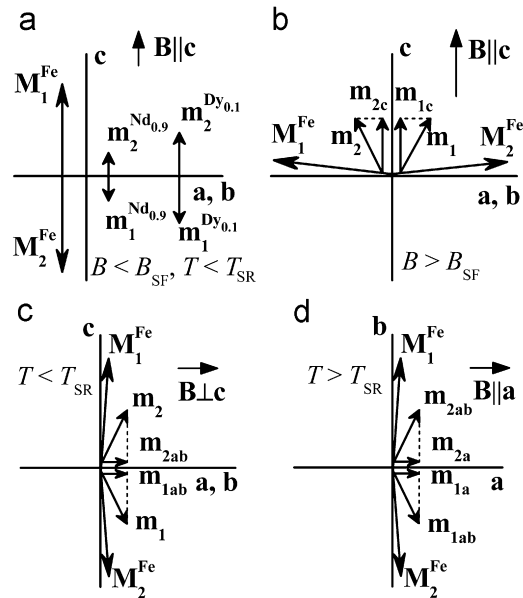

Fig. 1. Schemes of orientations of the magnetic moments of the iron M_i^{Fe} and rare-earth m_i^R sublattices used in the calculation of the magnetic characteristics of $Nd_{0.9}Dy_{0.1}Fe_3(BO_3)_4$ for different temperature ranges and different directions of the external magnetic field: (a, b) $B\|c$ (the ab plane is perpendicular to the figure plane), (c) $B\perp c$ (the ab plane are perpendicular to the figure plane), and (d) $B\|a$ (the c axis is perpendicular to the figure plane).

Table 1

Parameters of $Nd_{0.9}Dy_{0.1}Fe_3(BO_3)_4$ and for comparison also parameters of $NdFe_3(BO_3)_4$ [8] and $DyFe_3(BO_3)_4$ [5] (the intrachain Fe–Fe exchange field B_{dd1}, the interchain Fe–Fe exchange field B_{dd2}, and the f–d exchange field B_{fd} are the low-temperature exchange fields corresponding to the molecular constants λ_1, λ_2, and λ_{fd}^R, respectively; Δ_{fd} is the low-temperature splitting of the R ion ground-state due to the f–d interaction in the easy-plane (EP) $T=9$ K $> T_{SR}$ and easy-axis (EA) $T=2$ K $< T_{SR}$ states; Θ is the paramagnetic Neel temperature for the iron subsystem; $M_0 = |M_i(T=0, B=0)| = 15$ μ_B is the magnetic moment of iron per formula unit).

	$NdFe_3(BO_3)_4$ [8]	$Nd_{0.9}Dy_{0.1}Fe_3(BO_3)_4$	$DyFe_3(BO_3)_4$ [5]
$B_{dd1} = \lambda_1 M_0$, T	58	56	53
λ_1, T/μ_B	−3.87	–3.73	−3.53
$B_{dd2} = \lambda_2 M_0$, T	27	31	28
λ_2, T/μ_B	−1.8	−2.1	−1.87
$B_{fd} = \lambda_{fd}^R M_0$, T	7.1	12.7 (Nd)	3.3
		1.1 (Dy)	
λ_{fd}^R, T/μ_B	−0.47	–0.85 (Nd)	−0.22
		–0.07 (Dy)	
$\Delta_{fd} = \mu_B g|\lambda_{fd}|M_0$ cm^{-1}	8.8 (EP)	Nd	
		~8.8 (EA)	~ 19 (EA)
		~14.6 (EP)	
		Dy	
		~8.2 (EA)	
		~0.6 (EP)	
Θ, K	−130	−131	−180

Fig. 2. Experimental (symbols) and calculated (lines) magnetization curves of $Nd_{0.9}Dy_{0.1}Fe_3(BO_3)_4$ for B‖c and B⊥c at $T=2$ K. The inset shows magnetization curves $M_c(B)$ in fields up to 1.3 T at $T=2, 4, 5, 6, 7$ and 8 K.

Fig. 3. Experimental (symbols) and calculated (lines) magnetization curves of $Nd_{0.9}Dy_{0.1}Fe_3(BO_3)_4$ for several temperatures at B‖c. Calculated dashed curves show the contribution of the $Nd_{0.9}$, $Dy_{0.1}$ and Fe-subsystems to $M_c(B)$ at $T=15$ K.

magnetization curve is determined by the parameter λ_1 of the intrachain Fe–Fe exchange interaction, because the rotation of the magnetic moments of iron subsystem in the flop phase toward the field direction proceeds against this interaction. Using the two parameters (λ_{fd}^R and λ_1), we have calculated the magnetization curves $M_{c,\perp c}(B)$ at $T \leq 4$ K. Subsequent comparison to the experimental data allowed us to refine the parameters and provided a good agreement between experiment and theory for the entire set of magnetic characteristics (see Table 1). The parameter λ_2 enters into the Brillouin function, is responsible for the magnitude of the magnetic moment of iron at a given temperature and a given magnetic field, and determines the Neel temperature, because a three-dimensional order in the ferroborate structure is impossible without an exchange interaction between chains of the Fe^{3+} ions. The calculations also included the uniaxial anisotropy constant of iron $K_2 = 0.48$ T·μ_B (at $T=2$ K) and the anisotropy constant of iron in the basal plane $K_6 = -1.35 \times 10^{-2}$ T μ_B. With all these parameters we have calculated the magnetization curves $M_{c,\perp c}(B)$ in the fields up to 9 T at $T=2$–40 K and the temperature dependence of the initial magnetic susceptibility $\chi_{c,\perp c}(T)$ in a broad temperature range (2–300 K).

The magnetization data $M_{c,\perp c}(B)$ in Fig. 2 show a strong anisotropy at $T=2$ K. The anisotropy of the low-temperature magnetization curves $M_{c,\perp c}(B)$ in the ac plane is determined by the anisotropy of Nd^{3+} and Dy^{3+} ions. As can be seen from Fig. 2 the experimental and calculated curves $M_c(B)$ at $T=2$ K in a magnetic field $B_{SF} \approx 0.84$ T are characterized by a magnetization jump due to the spin-flop transition in the iron subsystem from the initial collinear phase (scheme (a) in Fig. 1) to the flop-phase (scheme (b) in Fig. 1). The rare-earth subsystem in the flop-phase is characterized by the magnetic moments in both sublattices m_i^R oriented along the field and significantly contributes to the jump in magnetization upon the spin-flop transition (the greatest contribution from the $Dy_{0.1}$ subsystem). The magnetic moments of the iron sublattices M_i^{Fe} are bent toward the field deviation from the ab plane.

As can be seen from the inset to Fig. 2, at $T < T = 8$ K the field of the spin-flop transition B_{SF} decreases with increasing temperature; i.e., with an increase in the temperature, the initial collinear
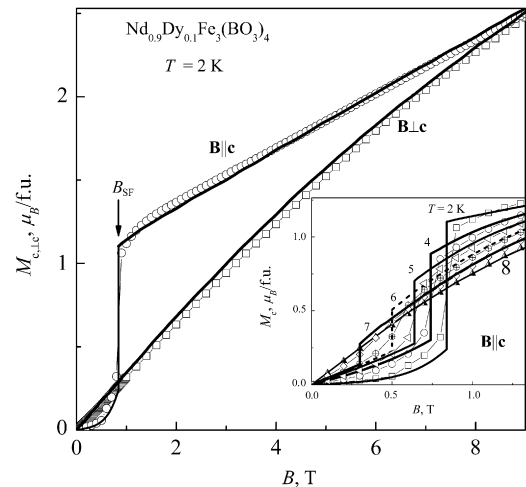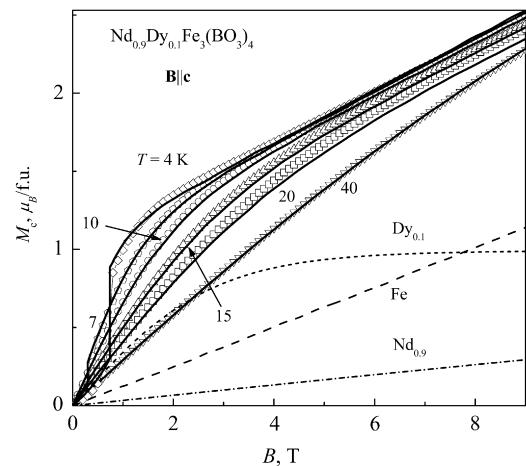
phase becomes less stable despite the increasing parallel component of the magnetic susceptibility of the iron subsystem. Thus, the observed dependence $B_{SF}(T)$ of $Nd_{0.9}Dy_{0.1}Fe_3(BO_3)_4$ compound differs from the corresponding dependences of $RFe_3(BO_3)_4$ with R=Tb [14,15], Nd [8], Dy [5] and Pr [16], in which the field of the spin-flop transition increases with increasing temperature, as it is often the case with uniaxial antiferromagnets. This behavior of the dependence $B_{SF}(T)$ of $Nd_{0.9}Dy_{0.1}Fe_3(BO_3)_4$ compound is associated with the fact that the temperatures of measurement of the magnetization curves $M_c(B)$ become closer to the spontaneous spin-reorientation transition temperature $T_{SR} \approx 8$ K. An increase in the temperature leads to a decrease in the contributions from the iron and rare-earth subsystems to the total effective magnetic anisotropy constant.

Experimental and calculated magnetization curves $M_{c,\perp c}(B)$ of $Nd_{0.9}Dy_{0.1}Fe_3(BO_3)_4$ at $T=4$–40 K are displayed in Figs. 3 and 4. As can be seen, there is a good agreement between experiment and theory at various temperatures, including the paramagnetic state at $T=40$ K. For comparison, Figs. 3 and 4 also show the contributions of the $Nd_{0.9}$, $Dy_{0.1}$ and Fe-subsystems (dashed curves) to $M_{c,\perp c}(B)$ at $T=15$ K.

It is interesting that in [12,18] for $Nd_{1-x}Dy_xFe_3(BO_3)_4$ ($x=0.15$, 0.25) a two-stage shape of the jump in the magnetization $M_c(B)$ at

[9] E.A. Popova, N. Tristan, C. Hess, et al., JETP 105 (2007) 105.
[10] M.I. Kobets, K.G. Dergachev, E.N. Khatsko, et al., Physica B 406 (2011) 3430.
[11] F. Yu., A.M. Popov, G.P. Kadomtseva, Vorob'ev, et al., JETP Lett 89 (2009) 345.
[12] I.A. Gudim, E.V. Eremin, V.L. Temerov, J. of Cryst. Growth 312 (2010) 2427.
[13] G.A. Zvyagina, K.R. Zhekov, I.V. Bilych, et al., Low Temp. Phys. 36 (2010) 279.
[14] E.A. Popova, D.V. Volkov, A.N. Vasiliev, A.A. Demidov, et al., Phys. Rev. B 75 (2007) 224413.

[15] D.V. Volkov, E.A. Popova, N.P. Kolmakova, A.A. Demidov, et al., J. Magn. Magn. Mater. 316 (2007) e717.
[16] A.A. Demidov, N.P. Kolmakova, D.V. Volkov, A.N. Vasiliev, Physica B 404 (2009) 213.
[17] A.A. Demidov, D.V. Volkov, Phys. of the Sol. St 53 (2011) 985.
[18] A.A. Demidov, I.A. Gudim, E.V. Eremin, JETP 114, N1 (in press).